Dust Destruction

James Guillochon

December 11, 2008

1. Introduction

The observed distribution of dust in the ISM is well-fitted by assuming the size distribution of the dust grains obeys a power law $dn \propto a^{-3.5}da$ (Mathis et al. (1977), hereafter the MRN distribution). Dust is primarily destroyed in supernova blast waves and other high temperature, high density environments, and these processes lead to destruction timescales of $\sim 5 \times 10^8$ years. In this report, we describe the various mechanisms for destroying dust in the ISM, and we summarize the results of numerical simulations that estimate the rate of dust destruction. Since the timescale for dust injection is approximately 2.5×10^9 years (Tielens 1990), we find that one predicts a far smaller fraction of dust depletion than indicated by extinction. This suggests that there must be an efficient process for converting gas back into dust that is not associated with the injection of dust into the ISM.

2. Destruction Mechanisms

Dust is converted to gas by colliding with other objects: Photons, gas, cosmic rays, and other grains, but not all of these interactions result in the destruction of dust. The mechanisms we are mostly interested in are the mechanisms that return matter from the dust phase to the gas phase. Processes such as grain cratering/shattering affect only the size distribution of dust, and these processes only have a first-order effect on the conversion of dust to gas by altering how those grains react to a shock.

2.1. Photons and Cosmic Rays

Photon-grain interactions produce a variety of different effects depending on the energy of the incident photon and the surface properties of the target dust grain (Jones 2004). Low-energy photons (radio and IR) are weakly absorbed by dust when the wavelength of the incident photon is larger than the dust grain itself. Photons in the visible to UV range can either be scattered off of dust grains or absorbed. If the photon is absorbed, the result of the interaction depends on whether the photon's energy is larger than the photoelectric work function ϕ of the material. A photon with an energy smaller than the work function energy will simply contribute to the thermal energy of the dust grain, and the grain re-radiates this energy as a blackbody at temperature T. If the photon has an energy larger than the work function, the kinetic energy of the emitted electron is simply $h\nu - \phi$. For most dust compositions, energies on the order of a couple eV are not enough to liberate surface atoms; that said, volatile materials like water ice have binding energies below an eV, and thus visible/UV photons are effective at destroying dust made from these materials. Photons with energies larger than $\gtrsim$ 5 eV can effectively remove surface atoms from most dust grains. If the flux is large enough, the fast removal of electrons can charge the grain and lead to the Coulomb expulsion of surface ions.

Cosmic rays are another potential dust destruction channel. Unfortunately, since Rutherford scattering is proportional to $v_{\rm cr}^{-3}$, the lowest energy cosmic rays will have the largest effect on dust grains. Since the Sun bombards us with cosmic rays in this energy range, we have no idea what the extrasolar cosmic ray spectrum looks like at these low energies. Their contribution to dust destruction remains an open question.

2.2. Sputtering

The primary mechanism for dust destruction is collisions with high-velocity ions ($v \geq 50$ km/s) in dense environments. These conditions are typically seen in the wakes of supernova blast waves. Gas-grain collisions, hereafter referred to as "sputtering," results in the direct conversion of matter from the dust phase to the gas phase. The number of atoms removed by an impacting ion with kinetic energy E is given by the following expression (Tielens et al. 1994).

$$Y = 4.2 \times 10^{14} \frac{\alpha S_n(E)}{U_0}, \tag{1}$$

where α is a function of the mass ratio of the impacting ion and the atoms that make up the projectile, $S_n(E)$ is a nuclear stopping cross section, and U_0 is the surface binding energy of the target grain. The actual sputtering yield is an average of this function over all possible impact angles

$$< Y > \equiv 2 \int_0^{\pi/2} Y \sin(\theta) \cos(\theta) d\theta. \tag{2}$$

For silicates, graphite, and iron, the surface binding energy is ~ 5 eV, whereas more volatile materials like ice have binding energies ~ 1 eV. Aside from volatiles, the sputtering rate is approximately the same for all materials. This means that the average velocity of the impacting ions on a given dust grain must be $\gtrsim 30$ km/s for sputtering to be effective.

We shall split sputtering into two separate categories: Thermal and non-thermal. Thermal sputtering refers to the case where $v_{\rm gas} \gg v_{\rm dust}$, and thus we can assume that the dust has zero velocity relative to the gas and thus interactions are isotropic. Non-thermal sputtering refers to the opposite extreme where $v_{\rm gas} \ll v_{\rm dust}$, and so in this case the dust is assumed to move in a fixed background of gas. The combination of these two limiting cases will give us the total contribution of sputtering to dust destruction.

Let's segue for a moment from our discussion of sputtering and focus on the environment sputtering is important, the wakes of supernovae. The Sedov-Taylor blast wave solution can be separated into three phases. The first phase describes the evolution of the blast wave immediately after detonation, in this phase the shock sweeps up very little mass and is considered to be in free expansion. In the second phase, the shell has expanded enough such that the mass swept up by the shock is comparable to the mass in the shock itself, this leads to an increase in density at the shock front. When the shock front becomes optically thin, the shell begins to radiatively cool.

During the third phase dust grains can be accelerated to the shock speed $v_{\rm sh}$ in a process known as "betatron" acceleration. The shocked gas behind a supernova blast wave rapidly cools, which leads to a compression of the gas. The gas is assumed to have an intrinsic magnetic field, and the condensation of the gas leads to an increase in the magnetic energy density. The change in magnetic field strength $\partial B/\partial t$ leads to an electromotive force which accelerates charged grain particles. This means that the dust energy will scale with the magnetic energy density (McKee et al. 1987).

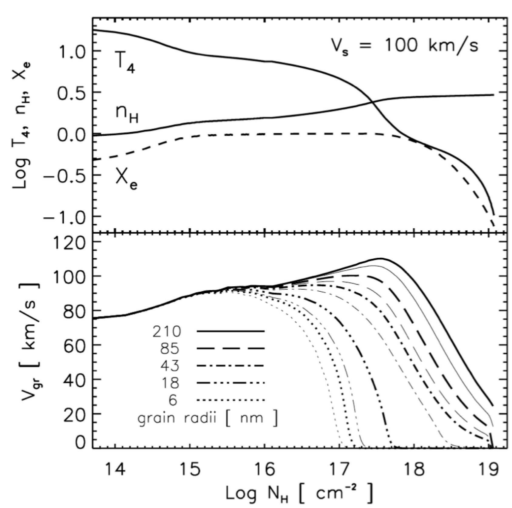

Fig. 1.— Velocity distribution of dust grains of various sizes at different column densities $N_{\rm H}$, figure from Jones (2004).

As long as grain charge scales with grain mass, grains of all sizes will be accelerated to the same velocity. However, the effects of drag depend on each grain's surface to mass ratio, $F_{\rm D} \sim (a\rho)^{-1}$. Thus, the larger dust grains are more difficult to decelerate and will have larger average velocities than the small dust grains (Figure 1). This means that non-thermal sputtering will destroy these grains preferentially, since the non-thermal sputtering yield

$$\frac{da}{dt} = \frac{m_{\rm sp}}{2\rho} v_g A < Y > n_{\rm H} \qquad (3)$$

is dependent on the grain velocity.

Thermal sputtering rates can be calculated by simply replacing E with $k_{\rm b}T$ in equation (2). Since post-shock temperature is proportional to $v_{\rm sh}^2$, thermal sputtering is only important in the fastest shocks ($\gtrsim 150$ km/s), with non-thermal sputtering dominated dust destruction processes for shocks with velocity between 50 and 150 km/s.

So where is sputtering the most effective? The ISM is modeled as a three-phase medium, each with different average densities and temperatures. The Hot Intercloud Medium (HIM) has temperatures of 5×10^5 K and densities of 0.003 cm^{-3}, the Warm Intercloud Medium (WIM) has temperatures of 10^4 K and densities of 0.25 cm^{-3}, and the Cold Neutral Medium (CNM) has temperatures of 80 K and densities of 40 cm^{-3}. These three phases have volume filling factors of 70-80%, 30%, and 2-4% respectively. If a supernova goes off in each of these phases, we wish to know which of the phases is the most conducive to dust destruction. The HIM is hot enough for thermal sputtering per ion to be significant, however the particle density is so low that gas-grain interaction is rare. The CNM has the opposite problem; while it is about a thousand times denser than the HIM and thus gas-grain interaction is common, SN shocks propagate very slowly through the thick background density and thus both betatron acceleration and heating of the ambient gas is minimal. The WIM is in a sweet spot of parameter space. Since it is 100 times denser than the HIM, gas-grain interaction is frequent, and SN shocks are capable of accelerating dust grain to high speed and heating the ISM significantly.

However, the cold phase of the ISM contains 90% of the dust mass. Therefore, one might expect that only a small fraction of the dust is capable of being destroyed. However, McKee (1989) showed that O star formation will reionize cold clouds on timescales of 3×10^7 years, significantly shorter than the dust destruction timescale. This means that all the dust in the CNM will be cycled to the WIM, and thus the cold phase cannot protect the dust.

2.3. Grain-grain Collisions

While gas-grain interactions are the primary dust destruction process, grain-grain collisions also play an important role. Grains can be vaporized by collisions with other grains, which converts dust back to the gas phase. Grains can also be shattered by collisions with other grains, this is *not* a destruction process as it merely redistributes the dust mass into grains of smaller sizes. Depending on the relative velocity between dust grains, a number of different things can happen. At velocities of $\sim$ 1 m/s, grains can stick together into aggregates; however this process leads to grains that are very easily disassociated because the geometry of the sticking surfaces are not very regular. At velocities of $\sim$ 20 m/s, dust grains harmlessly bounce off of each other. Collisions around 100 m/s can disassociate weakly bound aggregate grains, while collisions at 1 km/s can shatter grains of homogenous composition. At grain velocities of 20 km/s grains can be vaporized, but only the projectile is destroyed unless the grains are similar in mass.

Grain vaporization is less effective than sputtering for all but the largest grains. The gas yield from a given collision is maximized when the colliding grains are similar in size, and for large grains these events are rare since the number of large grains is small (as an example, there are 4×10^5 grains of 50Å in size for every 2000Å grain, assuming an MRN distribution). The threshold pressure required to shatter a grain is about $1/10^{\mathrm{th}}$ the vaporization critical pressure (Jones et al. 1996). This means that small grains are capable of shattering large grains, and since small grains are much more plentiful shattering events are much more common than vaporization events.

Let's consider what happens when a small grain impacts a large grain (Figure 2). A shock wave propagates both through the projectile and the target. Since the projectile is small, the shock wave reaches the opposite side of the projectile rapidly, and the impact completely vaporizes the smaller body. In the pressure range relevant to these collisions, the shock wave that propagates through the target splits into two waves with two different velocities. The first wave is "elastic" (stress and strain are linearly related) which applies the Hugoniot conditions to the post-shock material. The second wave is "plastic" (stress and strain are independent), this wave facilitates shearing motions and leads to permanent deformations such as the lip that forms around the crater. Rarefaction waves propagate from the free surfaces of the target, this creates a low-pressure region between the impactor and the compression wave. This allows material to flow out of the target grain. If the stresses exerted by this velocity field are larger than the shear strength, the material in the excavation zone will break up and result in the ejection of small dust grains. These grains follow a power law distribution with an exponent of -3.3 (Jones et al. 1996), with a maximum size roughly equal to the radius of the crater and a minimum size similar to the radius of the projectile.

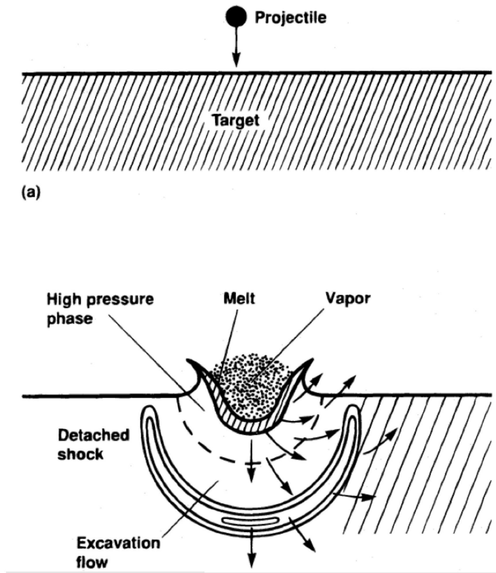

Fig. 2.— Crater formation in grain-grain collision, figure from Jones et al. (1996).

On average, half of the crater volume is ejected (of course, this is material-dependent).

If the post-shock pressure across most of the target grain is comparable to the tensile strength of the material, the target will be completely shattered; this is known as "catastrophic" destruction. When the shock waves reaches the back of the target grain, a rarefaction wave will propagate back into the grain and lead to nodes of high and low pressure that depend on the exact geometry of the grain. These maxima and minima lead to stress fractures which lead to the complete disruption of the grain. Since the threshold for shattering is so small, the largest grains (> 500Å) have lifetimes of only 10^7 years.

These events are important in terms of dust lifetime. Since smaller grains are more resistant to betatron acceleration, their differential velocities will be smaller than a distribution with many large grains. This means that both the non-thermal sputtering and grain vaporization processes will be less effective. Thus, the inclusion of grain shattering, perhaps counter-intuitively, increases the timescale of dust destruction processes.

3. Resultant Distribution

The process that dominates dust destruction depends heavily on the composition of the grain being destroyed and the velocity of the shock. For weak shocks (50 km/s), grain-grain collisions dominate the destruction rate, however the total fraction of dust destroyed is $\sim 1\%$.

For strong shocks (> 200 km/s), sputtering dominates destruction, with thermal sputtering being the most important destruction process for the smaller grains (Figure 3). The fraction destroyed in these shocks is closer to 50%.

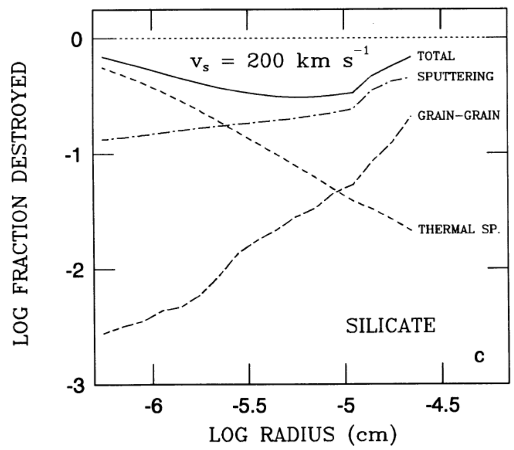

Fig. 3.— Fraction of silicate dust destroyed by a strong shock, figure from Jones et al. (1994).

Taking into account the effects of sputtering and grain-grain collisions, numerical simulations produce a distribution (Figure 4) which is self-similar to the initial power law distribution, with a slightly shallower exponent (-3.3). However, the distribution has been shifted to smaller grains, which leads to longer dust lifetimes.

From this figure, we can infer that the lifetime of dust is $\sim 5 \times 10^8$ years. This is longer than the lifetime of dust estimate without the effects of shattering (3×10^8 years), showing clearly that size distribution has a strong impact on dust lifetimes. Recall that the dust injection timescale is 3×10^9 years, almost an order of magnitude larger than the dust destruction timescale. Therefore, there must be some process that allows the observed dust depletion to be maintained.

A potential mechanism is the accretion of metallic ions onto small dust grains aided by Coulombic interactions, as suggested by Weingartner & Draine (1999). The timescale for this process is

$$\tau_a^{-1} = A^{-1/2} s \left(\frac{8\pi k_{\rm b} T}{m_{\rm p}}\right)^{1/2} \int a^2 \frac{dn_{\rm gr}}{da} D(a) da, \quad (4)$$

where A is the mass number of the ion, s is the "sticking" coefficient, a the grain radius, $n_{\rm gr}$ the number of grains with radius less than a, and $D(a)$ is a material-dependent constant. Weingartner found that this process can bring the dust abundance into equilibrium around the observed values even with efficient dust destruction. Another possibility suggested by Jones et al. (1994) is that non-volatile dust might accrete a mantle of more volatile material

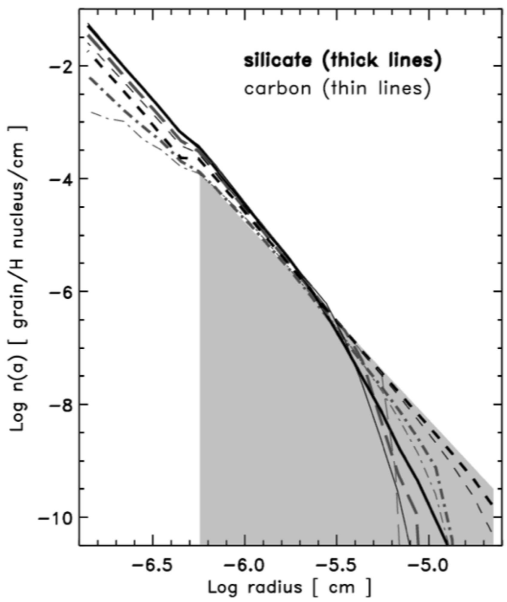

Fig. 4.— Resultant distribution including the effects of thermal/non-thermal sputtering, grain vaporization, and grain shattering, figure from Jones (2004).

that has a larger sticking coefficient. Additionally, the processing of the mantles by UV radiation can lead to the formation of organic compounds that can act as a glue to tightly bind aggregate grains. These aggregate grains have lower specific densities and are thus less betatron accelerated, resulting in higher survival rates. Unfortunately, this process alone is not enough to explain the observed dust depletion.

4. Conclusion

Thermal sputtering, non-thermal sputtering, and grain vaporization are efficient mechanisms that move metals from dust phase to gas phase, with each process dominating for different shock velocities. Grain shattering destroys large grains, but actually helps keep metals in the dust phase by reducing the yield from sputtering and grain-grain collisions. The timescale of dust destruction is short compared to the dust creation timescale, this suggests an efficient post-injection mechanism for converting gas into dust that is not yet fully understood.

REFERENCES

Biermann, P. & Harwit, M. 1980, ApJ, 241, L105, a&AA ID. AAA028.131.254

Borkowski, K. J. & Dwek, E. 1995, ApJ, 454, 254

Draine, B. T. 2003, A&A Rev., 41, 241

Jones, A. P. 2004, Astrophysics of Dust, 309, 347

Jones, A. P., Tielens, A. G. G. M., & Hollenbach, D. J. 1996, ApJ, 469, 740

Jones, A. P., Tielens, A. G. G. M., Hollenbach, D. J., & McKee, C. F. 1994, ApJ, 433, 797

Kemper, F., Vriend, W. J., & Tielens, A. G. G. M. 2004, ApJ, 609, 826

Liffman, K. & Clayton, D. D. 1989, ApJ, 340, 853

Mathis, J. S., Rumpl, W., & Nordsieck, K. H. 1977, ApJ, 217, 425, a&AA ID. AAA020.131.074

McKee, C. 1989, Interstellar Dust: Proceedings of the 135th Symposium of the International Astronomical Union, 135, 431

McKee, C. F., Hollenbach, D. J., Seab, G. C., & Tielens, A. G. G. M. 1987, ApJ, 318, 674

Routly, P. M. & Spitzer, L. 1952, ApJ, 115, 227

Tielens, A. G. G. M. 1990, In its Carbon in the Galaxy, 59

—. 1998, ApJ, 499, 267

—. 2005, The Physics and Chemistry of the Interstellar Medium, iSBN: 0521826349

Tielens, A. G. G. M., McKee, C. F., Seab, C. G., & Hollenbach, D. J. 1994, ApJ, 431, 321

Weingartner, J. C. & Draine, B. T. 1999, The Astrophysical Journal, 517, 292, (c) 1999: The American Astronomical Society

Wood, K., Wolff, M. J., Bjorkman, J. E., & Whitney, B. 2002, ApJ, 564, 887
